Magnetoreflectivity study of the band structure of $Hg_{1-x}Mn_xTe$ ($0.026 \leq x \leq 0.106$)

G. Bauer
Institut für Physik, Montanuniversität Leoben, A-8700 Leoben, Austria

J. Kossut
Institute of Physics, Polish Academy of Sciences, Pl-02668 Warszawa, Poland

R. Faymonville and R. Dornhaus
I. Physikalisches Institut der Rheinisch-Westfälischen Technischen Hochschule Aachen, D-5100 Aachen, Federal Republic of Germany

(Received 9 July 1984)

The reflectivity of semimagnetic $Hg_{1-x}Mn_xTe$ samples has been measured in magnetic fields up to 5 T at $T=5$ K for $x=0.026$, 0.035, 0.05, and 0.106. This range of compositions has not been previously investigated systematically by magneto-optical methods. Measurements in the far-infrared frequency range 30—400 cm^{-1} were performed using Fourier-transform spectroscopy. The magnetization of two of the samples has also been measured. The magneto-optical transitions observed have been interpreted in terms of the modified Pidgeon-Brown model including exchange terms. Pinning effects were observed when the transition energies in Faraday and Voigt configurations became comparable with one of the longitudinal-optic-phonon energies.

I. INTRODUCTION

Semimagnetic semiconductors or diluted magnetic semiconductors are usually ternary semiconducting compounds whose lattice is made up in part of substitutional magnetic ions. The presence of these ions leads to localized spin moments and consequently leads to an exchange interaction between these localized magnetic moments and the band electrons. The importance of this interaction has been discussed in several review articles.[1-5]

Several magneto-optical investigations of the typical semimagnetic compound $Hg_{1-x}Mn_xTe$ have been reported so far.[6-11] These investigations dealt mainly with samples with compositions x ranging from 0 to 0.02 and from 0.12 to 0.15.[6-9] To our knowledge there are only two papers where the magneto-optical properties of materials with $x \cong 0.1$ (Refs. 10 and 11) were studied.

For materials with $0.02 < x < 0.1$, the magneto-optical properties have to be studied using far-infrared radiation (both for intraband as well as interband transitions) since the semimetal-to-semiconductor transition of the Γ_6- and Γ_8-level crossover occurs in $Hg_{1-x}Mn_xTe$ at $x=0.07$ of 5 K.[5,9]

In Ref. 10, due to the rather short wavelength of radiation used, only weak magneto-optical interband transitions could be observed for $x \cong 0.1$. Stronger transitions (e.g., cyclotron resonance or spin resonance) could not be observed because of the limitation of the magnetic field strength available.

Optical properties of $Hg_{1-x}Mn_xTe$ with $x=0.06$ were studied at zero magnetic field with reflectivity measurements by McKnight *et al.*[12] Other compositions were also studied by Gebicki *et al.*,[13] where the main interest was concentrated on the optical-phonon energies in these crystals, and by Kaniewski and Mycielski[14] in absorption.

Magneto-optical measurements proved to be more accurate than, e.g., Shubnikov—de Haas experiments[15-17] as far as the determination of the relevant band parameters is concerned. Therefore, in the present work, the magnetoreflectivity of samples with x ranging from 0.026 to 0.106 was studied in order to fill, at least partially, the gap in the composition studied by optical methods. The Fourier-transform spectroscopy technique was employed. The data obtained in this way were analyzed in conjunction with the magnetization values measured in the same samples as studied by optical methods. Since the electronic energy levels in semimagnetic $Hg_{1-x}Mn_xTe$ crystals are modified strongly by the exchange interaction between conduction or valence electrons and localized $3d$ electrons of Mn ions and the modification proves to be proportional to the magnetization, the knowledge of the magnetization was an advantage in the present study. Thus we believe that we were able to establish the values of the relevant exchange constants α and β less ambiguously than in other magneto-optical studies, where the magnetization was only determined indirectly.

II. EXPERIMENTAL

The samples used in the present investigation were grown by the modified Bridgman method. The composition of the crystals was $x=0.026, 0.035, 0.05, 0.106$. The Mn content was determined for all alloy compositions by density measurements. In addition, the composition was checked by the determination of the lattice constants by means of x-ray diffraction. The variation of lattice constant with composition was found to be in reasonable agreement with composition was found to be in reasonable agreement with that given by Delves and Lewis.[18] Some of the samples were annealed in Hg vapor to reduce the

number of Hg vacancies. In all samples investigated, the position of the Fermi level was close to the Γ_8 level (inverted-band scheme) or to the Γ_6 level ($x=0.106$ sample).

Prior to the magneto-optical reflectivity measurements, the samples were mechanically polished and chemically etched in bromine methanol solution. The reflectivity measurements were performed using Fourier-transform spectroscopy (a rapid-scan interferometer, Bruker IFS 113, with attached high-vacuum chamber for cryostat with superconducting magnet was used) in the frequency range 30—400 cm^{-1}. The samples were kept in the insert of the split coil magnet allowing measurements in Faraday ($\mathbf{B}||\mathbf{k}$) and Voigt geometry ($\mathbf{B}\perp\mathbf{k},\mathbf{B}||\mathbf{E}$, $\mathbf{B}\perp\mathbf{E}$, $\mathbf{E}$ denoting the electric field vector of radiation, $\mathbf{k}$ the propagation direction of electromagnetic radiation) in magnetic fields B up to 5 T. In the case of Faraday geometry, the incident radiation was unpolarized (circularly polarized radiation cannot be used in Fourier-transform spectroscopy) whereas in Voigt geometry linearly polarized radiation, either along the direction of B or perpendicular to it, was used. A liquid-helium-cooled Ge bolometer was used as a detector. The accuracy of the reflectivity measurements was better than 2%. The magnetization measurements of $x=0.026$ and 0.5 samples were performed in fields up to 15 T at temperatures $T=1.9$ and 4.2 K.

III. RESULTS

A. Magneto-optical data

The magneto-optical reflectivity spectra are exemplified for the $x=0.026$ and 0.05 samples in Figs. 1 and 2 for the two Voigt configurations ($\mathbf{E}\perp\mathbf{B},\mathbf{E}||\mathbf{B}$). Similar results were obtained for the other samples at $T=5$ K. It is clearly seen that in addition to the two dominant structures caused by the infrared-active phonon modes, the reflectivity is modulated apparently by electronic transitions, the energy of which depends on the applied magnetic field.

The reflectivity spectra are determined by the frequency- and magnetic-field-dependent dielectric function. Apart from $\epsilon_\infty=1+\chi_\infty$ (the high-frequency dielectric constant) and the two-phonon oscillators, the excitation of electrons from the Landau levels in the valence band to those of the conduction band (interband transitions) as well as within one Landau-ladder system (intraband transitions) will contribute to the total dielectric function.

The magnetic-field- and frequency-dependent reflectivity can be analyzed either by assuming a model dielectric function and fitting its parameters to the experimentally observed data, or by a direct Kramers-Kronig analysis of the reflectivity data. Assuming $\mathbf{B}||z$, then in the Voigt configuration for $\mathbf{E}||\mathbf{B}$ the complex refractive index $\tilde{n}^2$ is determined by $\tilde{n}_{||}^2=\epsilon_{zz}$, whereas for the $\mathbf{E}\perp\mathbf{B}$ configuration, $\tilde{n}_{\perp}^2=\epsilon_\perp=\epsilon_{xx}+\epsilon_{xy}/\epsilon_{zz}$.

In order to obtain the magneto-optical transition energies, for all samples the imaginary part of ϵ, $\mathrm{Im}[\epsilon(\tilde{\nu},B)]=\epsilon''$, the real part ϵ' as well as $\mathrm{Im}(-1/\epsilon)$ were determined. As an example, plots of these quantities are

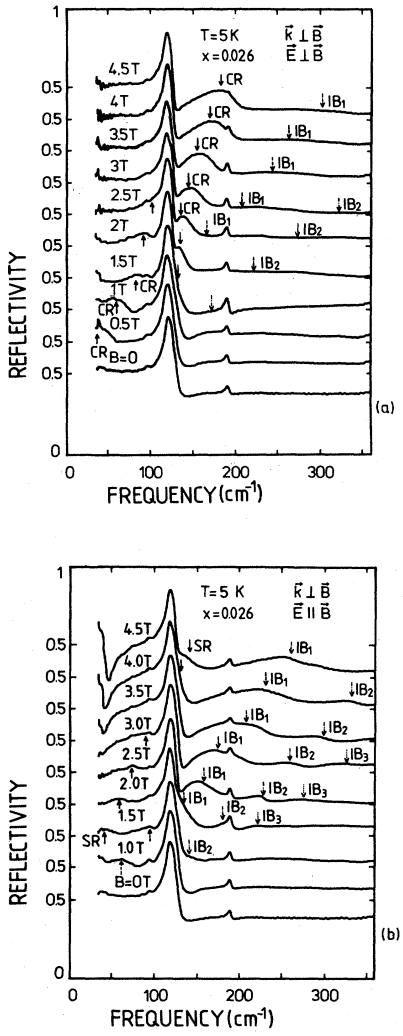

FIG. 1. The magnetoreflectivity of $Hg_{1-x}Mn_xTe$, $x=0.026$, in various magnetic fields in (a) Voigt $\mathbf{E}\perp\mathbf{B}$ geometry and (b) $\mathbf{E}||\mathbf{B}$ configuration. Arrows indicate the following transitions: (a) CR, $a_c(0)\rightarrow a_c(1)$; IB_1, $a_v(2)\rightarrow a_c(1)$; IB_2, $a_v(3)\rightarrow a_c(2)$. (b) SR, $a_c(0)\rightarrow b_c(0)$; IB_1, $b_v(2)\rightarrow a_c(1)$; IB_2, $a_v(-1)\rightarrow b_c(1)$; IB_3, $b_v(3)\rightarrow a_c(2)$.

shown in Figs. 3 and 4 for the composition $x=0.026$, where $\mathrm{Im}\epsilon$ and $\mathrm{Im}(-1/\epsilon)$ for various magnetic fields as a function of wave number $\tilde{\nu}$ are given. Since $Hg_{1-x}Mn_xTe$ exhibits a two-mode behavior,[13] the structures at 118 and 190 cm^{-1} (in $\mathrm{Im}\epsilon$) are due to HgTe-like and MnTe-like transverse optic (TO) phonon modes. An additional mode at 95—98 cm^{-1}, already observed by McKnight *et al.*[12] (for $x=0.06$), is probably associated with a defect not present in HgTe. Not all magneto-optical transitions observed in the magnetoreflectivity spectra are of the same oscillator strength. Thus weak transitions observable as weak structures on the originals of ϵ'' and ϵ' are difficult to reproduce in an overall representation. A precise determination of the position of transitions with small oscillator strength is not directly possible using the reflectivity data but much more reliable if

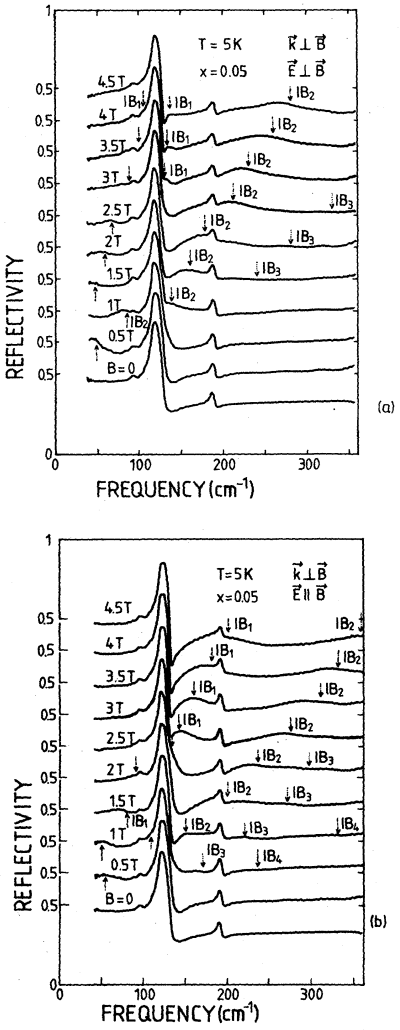

FIG. 2. As Fig. 1 but for $Hg_{1-x}Mn_xTe$, $x=0.05$. (a) IB_1, $a_v(-1)\rightarrow a_c(0)$; IB_2, $b_v(-1)\rightarrow b_c(0)$; IB_3, $a_v(-1)\rightarrow a_c(1)$. (b) IB_1, $b_v(1)\rightarrow a_c(0)$; IB_2, $a_v(-1)\rightarrow b_c(0)$; IB_3, $b_v(+2)\rightarrow a_c(1)$; IB_4, $b_v(3)\rightarrow a_c(2)$.

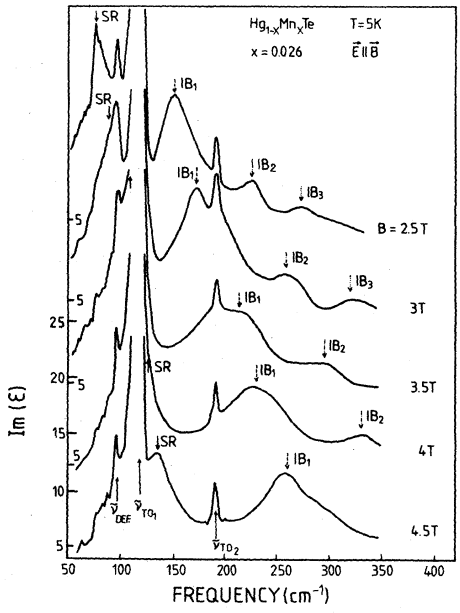

FIG. 3. Imaginary part of dielectric function vs frequency obtained by Kramers-Kronig analysis from the reflectivity data presented in Fig. 1. ($Hg_{1-x}Mn_xTe$, $x=0.026$ at $T=5$ K) for various magnetic fields ($\tilde{\nu}=118$ and 190 cm^{-1}, HgTe- and CdTe-like TO-phonon modes; peak value of $Im\epsilon$ at $\tilde{\nu}=118$ cm^{-1}, ≈ 200; third stationary mode at $\tilde{\nu}=95$ cm^{-1}, probably defect mode). Arrows indicate the following transitions: SR, $a_c(0)\rightarrow b_c(0)$; IB_1, $b_v(2)\rightarrow a_c(1)$; IB_2, $a_v(-1)\rightarrow b_c(1)$; IB_3, $b_v(3)\rightarrow a_c(2)$.

the Kramers-Kronig transformed curves are used (see Figs. 1 and 3).

Since the real and imaginary part of the frequency-dependent dielectric function were obtained by the Kramers-Kronig analysis of the reflectivity data, we did not perform (with the exception of the $x=0.106$ sample) an additional oscillator fit to reproduce the measured reflectivity data as described, e.g., in Refs. 19 and 20. Instead, the interband magnetooptical transition energies were assumed to correspond closely to the extrema of $Im\epsilon$ (Refs. 19 and 20) as a function of ω, as the absorption is mainly determined by $Im\epsilon$. Possible shifts of the real resonance energies away from the maxima of $Im\epsilon$ are discussed, e.g., by Aggarwal[19] and Weiler[20] for a simple-model dielectric function for magneto-optical interband transitions using parabolic bands.

Apart from the broadening effects due to finite collision time τ, the complications of the Γ_8 heavy-hole Landau-level spectrum of semimagnetic $Hg_{1-x}Mn_xTe$ as function of k_z enter into a model calculation for the dielectric function, because the combined density of states will not have extremal values for $k_z=0$ for all values of x and magnetic fields used. Due to these complications, no attempt was made to reproduce the dielectric function as obtained by the Kramers-Kronig analysis by a model calculation which would have been worthwhile only for the realistic Landau-level structure and the wave functions of $Hg_{1-x}Mn_xTe$.

The observed lines are sometimes broad, particularly in the region close to the phonon lines, and we always indicate their width as vertical error bars in the fancharts. A detailed analysis of the line shape would require, particularly in the vicinity of the phonon lines, further investigations. The position of the transitions obtained in a way described above proved to be (see next section) in agreement with a direct numerical classical oscillator fit of the reflectivity curves, at least for intraband transitions using the expressions, e.g., given by Palik and Furdyna[21] (see also Ref. 22).

With the application of a magnetic field, several magneto-optical transitions appear with apparently different selection rules in $\mathbf{E}||\mathbf{B}$ and $\mathbf{E}\perp\mathbf{B}$ geometry (see Figs. 1 and 2). To analyze the origin and position of these transitions, detailed information concerning the electronic energy levels in quantizing magnetic fields is required.

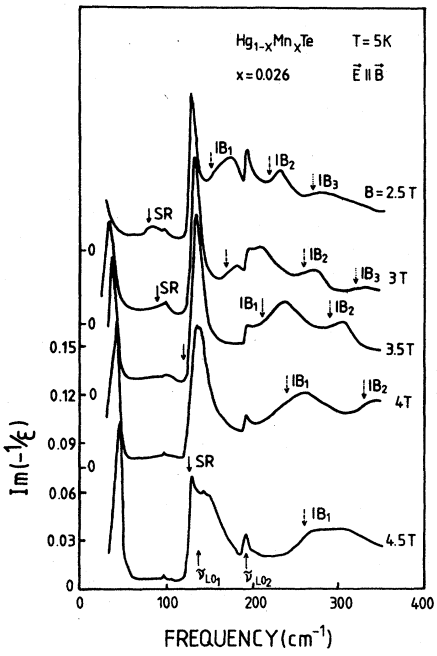

FIG. 4. Im$(-1/\epsilon)$ vs frequency for $x=0.026$ sample for various magnetic fields (arrows indicate transitions as in Fig. 3).

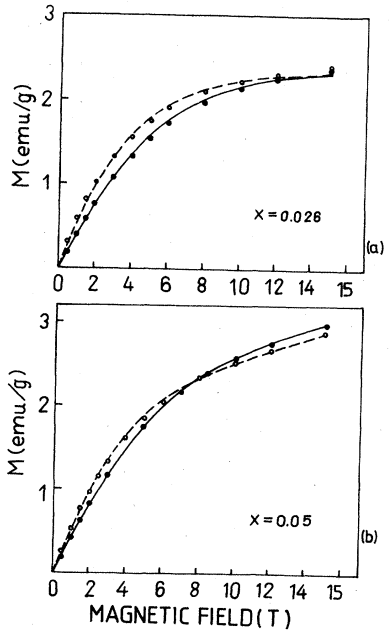

FIG. 5. Magnetization in $Hg_{1-x}Mn_xTe$ for (a) $x=0.026$ and (b) $x=0.05$ at $T=1.9$ K (open circles) and $T=4.2$ K (solid circles). The fit of the modified Brillouin function to the data is shown by solid ($T=4.2$ K) and broken ($T=1.9$ K) lines.

B. Magnetization

The magnetization of $Hg_{1-x}Mn_xTe$ in high magnetic fields was measured only for few values of x.[23] Therefore the magnetization of the $x=0.026$ and 0.05 samples at $T=1.9$ and 4.2 K are shown in Figs. 5(a) and 5(b), respectively.

The modified Brillouin function[24]

$$S_0 B_{5/2}\frac{2\mu_B B}{k_B(T+T_0)} \tag{1}$$

was fitted to the experimental magnetization data at both temperatures T. The parameters of the fit were obtained to be as follows: for the $x=0.026$ sample, $S_0=2.77$, $T_0=8$ K (at $T=4.2$ K), and $S_0=2.67$, $T_0=5.4$ K (at $T=1.9$ K); for the $x=0.05$ sample, $S_0=1.88$, $T_0=8.2$ K (at 4.2 K), and $S_0=1.68$, $T_0=7.4$ K (at $T=1.9$ K). This represents an overall fit for the whole range of magnetic fields. The values of S_0 for the $x=0.026$ sample are greater than 2.5, which seems to be in contradiction with the antiferromagnetic character of Mn-Mn coupling. If one fixes S_0 to be equal to 2.5, then one obtains the value of T_0 equal to 4.3 K (at $T=4.2$ K). The quality of the fit is comparable to the one given, if the fields are not higher than 6 T. For the whole range of fields no comparable quality can be found when S_0 is limited to values smaller than 2.5. However, treating S_0 just as a fit parameter, any description of the experimentally measured magnetization is acceptable.

It must be stressed that the magnetization gives the information about the product S_0 and the crystal composition parameter x. Therefore, in order to extract S_0 one has to know precisely the value of x. Fortunately in the band-structure description there is also only this product involved. For instance if the x value is changed from 0.026 to 0.029 one is bound to change the S_0 value from 2.77 to 2.48, which is already smaller than 2.5 as required by simple physical reasoning. However, such a precise knowledge of x is not possible when one relies on its determination by the density method or lattice-constant measurements. On the other hand, a rather steep dependence of the energy gap on x (and thus of the effective mass on x) allows the determination of the composition of the crystal in a more precise way whenever a cyclotron transition is observable (the mass is only very slightly affected by the exchange interaction and thus is insensitive to the magnetization). This was exactly the manner in which we established the value of $x=0.026$ in one of our samples. This, in turn, leads to "unphysical" value of $S_0=2.77$ for this sample.

Furthermore, the value of S_0 (or rather xS_0) is determined by the magnetization in an unambiguous way, provided that a large portion of its saturation is observed. However, in the case of the $x=0.026$ sample, only the beginning of the saturation region is covered. Therefore there is an uncertainty in the S_0 determination (one can observe that the quality of the fit decreases in the highest magnetic field region). Fortunately, our magneto-optical study is limited to smaller magnetic fields where the fit is much better but less sensitive to the actual choice of S_0 allowing, with equal confidence level, for physically plausible values S_0 smaller than 2.5, as mentioned above.

IV. ANALYSIS OF THE MAGNETO-OPTICAL RESULTS

The interpretation of the optical measurements was based on the model of the band structure of a narrow-gap semiconductor containing localized magnetic moments.[2] The model consists essentially of two parts. The first takes into account the $\mathbf{k}\cdot\mathbf{p}$ interaction between closely spaced energy levels $\Gamma_6,\Gamma_8,\Gamma_7$ [via interband momentum matrix element P ($\epsilon_{\Gamma_6}-\epsilon_{\Gamma_8}=E_g$; $\epsilon_{\Gamma_8}-\epsilon_{\Gamma_7}=\Delta$)] and also the spin-orbit interaction. The interaction of these levels with more remote bands is described in a perturbative way by means of the parameters γ_1, γ_2, γ_3, κ, and F. The second part of the model accounts for (in the mean-field approximation) the exchange interaction between electrons in the $\Gamma_6,\Gamma_7,\Gamma_8$ levels with localized magnetic moments due to $3d$ electrons of Mn ions. This interaction introduces two exchange constants: α (for Γ_6 or s-like electrons) and β (for Γ_8,Γ_7 or p-like electrons). This part contains the information about the magnetization of the sample. The solution of the model gives energies of Landau levels in the conduction, heavy-hole, light-hole, and spin-orbit split-off band. The solutions fall into two categories (named usually a and b sets) corresponding roughly to spin-up and -down levels. It is also a characteristic feature of this part that it mainly modifies only the spin properties of the conduction and valence electrons (i.e., it affects the electronic g^*-factor values), leaving their effective masses only slightly perturbed and determined basically by the $\mathbf{k}\cdot\mathbf{p}$ part or the model (the Pidgeon-Brown model). Therefore, the optical transition energies in the $\mathbf{E}\perp\mathbf{B}$ configuration are only weakly dependent on the magnetization of the sample since they involve the transitions within the same set of solutions (a to a or b to b, e.g., the cyclotron resonance). On the other hand, the energies of optical transitions in the $\mathbf{E}||\mathbf{B}$ configuration involving different sets of Landau levels (a to b or b to a, e.g., the spin resonance) will be very sensitive to the actual magnetization of a sample.

The analysis of the optical transitions in the $\mathbf{E}\perp\mathbf{B}$ configuration allowed us to determine the values of E_g and P (the effective mass of conduction electrons $m^*\sim E_g/P^2$) and thus provided a rather accurate determination of the concentration x of Mn ions (from the E_g-vs-x relationship in Ref. 25), more accurate than chosen values as obtained by the density method and lattice-constant investigation. The corresponding fan charts are given in Figs. 6(a), 7, 8(a), and 9 for $x=0.026$, 0.035, 0.05, and 0.106, respectively, together with the assignment of the levels between which the transitions occur. The theoretical transition energies plotted in these figures were calculated using the band parameters listed in Table I. The observed transitions in the $\mathbf{E}\perp\mathbf{B}$ configuration are consistent with the selection rules [$a(n)\rightarrow a(n\pm1)$ or $b(n)\rightarrow b(n\pm1)$] (according to Ref. 26) with the exception of a weak line observed in the $x=0.05$ sample which involves a change in the Landau quantum number n by 2. Such transitions are weakly allowed by the lack of the inversion symmetry in zinc-blende structure materials.[26]

Similarly, the transitions observed in the $\mathbf{E}||\mathbf{B}$ configuration agreed overall with the selection rules for this case

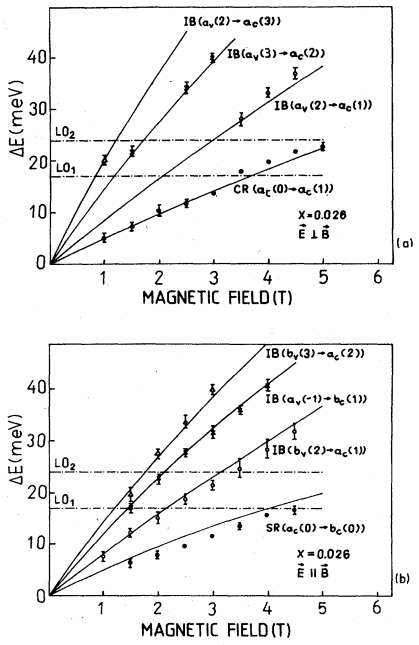

FIG. 6. Theoretical (lines) and experimental (symbols) magneto-optical transitions energies observed in (a) $\mathbf{E}\perp\mathbf{B}$ configuration and (b) $\mathbf{E}||\mathbf{B}$ configuration in $Hg_{1-x}Mn_xTe$ with $x=0.026$ at 5 K. The initial and final electronic states for each transition are indicated. (CR, cyclotron resonance; IB, interband transition; SR, spin resonance). The horizontal lines show the energies of LO phonons (LO_1 for HgTe-like mode and LO_2 for MnTe-like mode).

[$a(n)\rightarrow b(n+1)$ or $b(n)\rightarrow a(n-1)$], with the exception of a very weak line observed in $x=0.026$ sample. It again involved a transition between Landau levels with quantum numbers n differing by 2 which, as before, is weakly allowed when the breaking of the main selection rules by the lack of inversion symmetry is taken into account. The fan charts for the transitions observed in $\mathbf{E}||\mathbf{B}$ configuration in $x=0.026$ and 0.05 samples are given in Figs. 6(b) and 8(b), respectively.

As mentioned before, the theoretical transition energies in $\mathbf{E}||\mathbf{B}$ geometry are sensitive to the values of the exchange constants α,β, and the value of the magnetization.

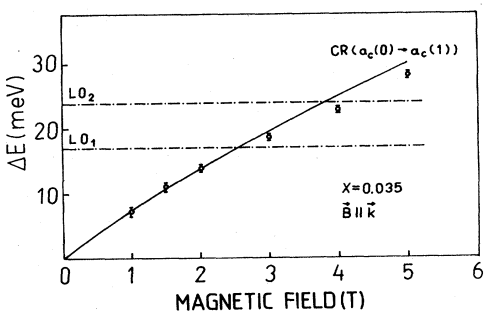

FIG. 7. Cyclotron-resonance energies in $Hg_{1-x}Mn_xTe$ ($x=0.035$) observed (symbols) in the Faraday configuration and calculated (solid line) at 5 K.

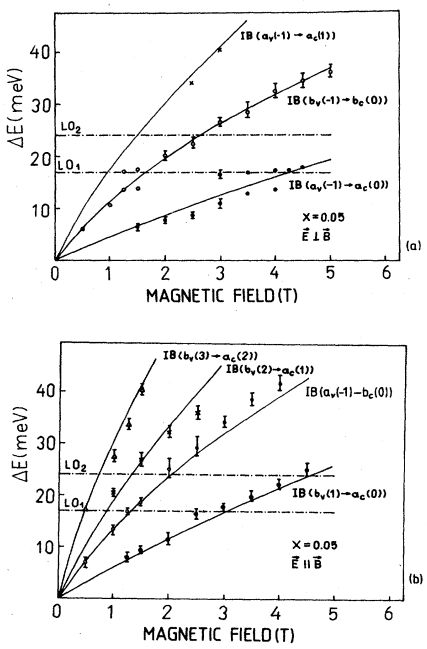

FIG. 8. Theoretical (lines) and experimental (symbols) optical transition energies for $Hg_{1-x}Mn_xTe$ ($x=0.05$) at $T=5$ K in (a) $\mathbf{E}\perp\mathbf{B}$ and (b) $\mathbf{E}\|\mathbf{B}$ configurations.

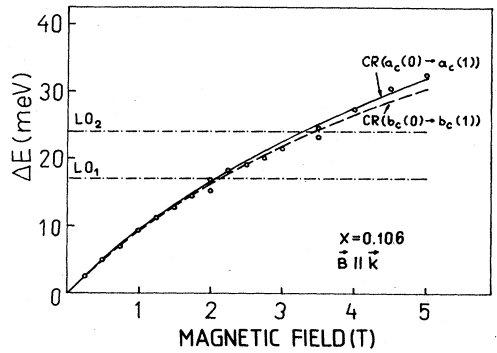

FIG. 9. Cyclotron-resonance energies in $Hg_{1-x}Mn_xTe$ ($x=0.106$) observed (points) and calculated (lines) at $T=5$ K. The CR in the a Landau ladder (solid line) and in the b Landau ladder (broken line) are shown. Both transitions are very close because of a reduction of the electronic g^* factor by the exchange interaction. Below 1 T the experimental transition energies correspond to $a_c(1)\rightarrow a_c(2)$ or $b_c(1)\rightarrow b_c(2)$.

Since the latter was taken from an independent experiment, carried out on the same samples, we were able to establish rather precisely the values of α and β. We found that the values of these constants obtained in Ref. 8, namely $\alpha=-0.4$ eV and $\beta=0.6$ eV, describe the present data well. It should be mentioned that the carrier concentrations (given also in Table I) as estimated from the observed positions of the plasma edge yield the values of the Fermi levels which are consistent with the assignment of the observed lines to the initial and final Landau levels.

For the n-type $x=0.026$ sample the transition $b_v(-1)\rightarrow b_c(0)$, possible in the $\mathbf{E}\perp\mathbf{B}$ case, from the consideration of the Fermi-level position, would be practically indistinguishable from the cyclotron resonance $a_c(0)\rightarrow a_c(1)$ indicated in Fig. 6(a).

On the other hand, the Fermi level in the p-type $x=0.05$ sample is very close to the bottom of the $b_v(-1)$ level (≈ 0.5 meV below it). For $k_BT\approx 0.5$ meV at $T=5$ K, this level is not completely depopulated and is therefore still an initial state for interband transitions. In addition this level has a large density of states even away from its top ($k_z=0$) and moreover has a camel-back shape in k_z. So even transitions starting at $k_z\neq 0$ can be strong enough to be observable.

In the case of all samples studied, the magneto-optical transitions indicated the existence of a pinning effect due to LO-phonon–electron interaction. The LO-phonon energies were obtained from Kramers-Kronig analysis of reflectivity by calculation of $\mathrm{Im}(-1/\epsilon)$ and are given also in Figs. 6–9. It is worthwhile noting that the pinning effect is observed here in the interband magneto-optical transitions also. There are only few observations of the pinning in such a case reported up to now.[27,28]

The Landau levels versus magnetic field in the $x=0.026$, 0.035, 0.05, and 0.106 samples are plotted in Figs. 10, 11, 12, and 13. It can be seen that only in the case of the $x=0.026$ sample does the band overlap between the $b_v(-1)$ and $a_c(0)$ states exist. In the cases of the $x=0.35$ and 0.05 samples, the uppermost valence-band level $b_v(-1)$ is below the lowest conduction-band level $a_c(0)$. This is in contradiction to the results of Ref. 17. The energetic distance ΔE between the $b_v(-1)$ and $a_c(0)$ levels depends on the magnetic field (and is positive if there is an overlap), can be calculated analytically (assuming $\Delta=\infty$), and is given by

$$\Delta E=\tfrac{1}{2}\left[x\,|\langle S_z\rangle|\left[\frac{\alpha}{2}+\frac{5\beta}{6}\right]-E_g+\frac{\hbar eB}{m_0c}(2\gamma_1-4\gamma_2+2\kappa-F-1)\right.$$
$$\left.-\left\{\left[E_g+\frac{\hbar eB}{m_0c}(F+1+\tfrac{3}{2}\gamma_1-\tfrac{3}{2}\gamma_2-\tfrac{1}{2}\kappa)+\tfrac{1}{2}x\langle S_z\rangle\left[\alpha+\frac{\beta}{3}\right]\right]^2+\frac{4eB}{3m_0c}P^2\right\}^{1/2}\right]. \quad (2)$$

The upward shift of the $b_v(-1)$ level (which produces the band overlap) is due to the exchange interaction effect and therefore is greater if the magnetization is larger. One has to remember that the antiferromagnetic interaction, which couples the localized magnetic moments in $Hg_{1-x}Mn_xTe$, tends to reduce the actual magnetization at a given magnetic field from the value that can be expected for a noninteracting spin system. Therefore, it is very easy to overestimate the magnetization, if no direct experimental information on this quantity is available. Overes-

TABLE I. Band-structure parameters of $Hg_{1-x}Mn_xTe$.

x	Type	$n(p)$[a] (cm^{-3})	E_g[b] (meV)	P[c] (eV cm)	Δ[c] (eV)	γ_1[c]	$\gamma_2=\gamma_3$[c]	κ[c]	F	α[b] (eV)	β[b] (eV)	S_0	T_0 (K)
0.026	n	1×10^{16}	−170	8.1×10^{-8}	1.08	3	0.25	−1.65	0	−0.4	0.6	2.77[b]	5.8[b] (at 4.2 K)
0.035	n	$<7\times10^{15}$	−125	8.05×10^{-8}	1.08	3	0.25	−1.65	0	−0.4	0.6	2.67[b]	5.4[b] (at 1.9 K)
0.05	p	3×10^{15}	−70	8.0×10^{-8}	1.08	3	0.25	−1.65	0	−0.4	0.6	2.40[d]	7.0[d] (at 4.2 K)
0.106	n	1×10^{16}	107	7.5×10^{-8}	1.08	5	1.5	−0.5	0	−0.4	0.6	1.88[b]	8.2[b] (at 4.2 K)
												1.68[b]	7.4[b] (at 1.9 K)
												1.02[e]	8.6[e] (at 4.2 K)

[a]Estimated, based on the position of the plasma edges observed in reflectivity.
[b]Based on measurements presented in this paper.
[c]From Ref. 8.
[d]Interpolation between available data.
[e]From Ref. 23.

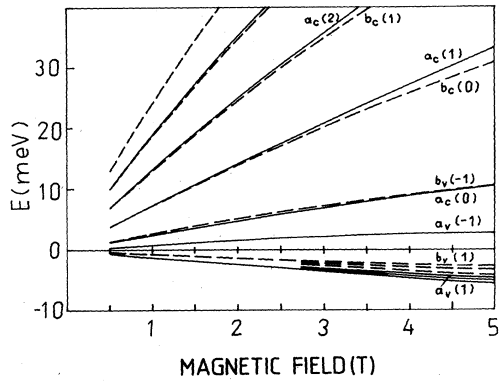

FIG. 10. Landau levels in the conduction and heavy-hole bands calculated at 5 K (a set, solid lines; b set, broken lines) for $x=0.026$.

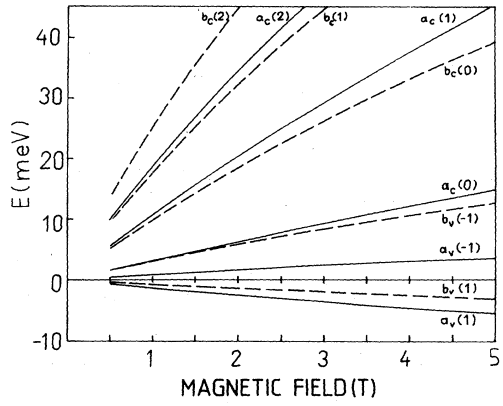

FIG. 11. Same as for Fig. 10 for $x=0.035$ (Note absence of the band overlap).

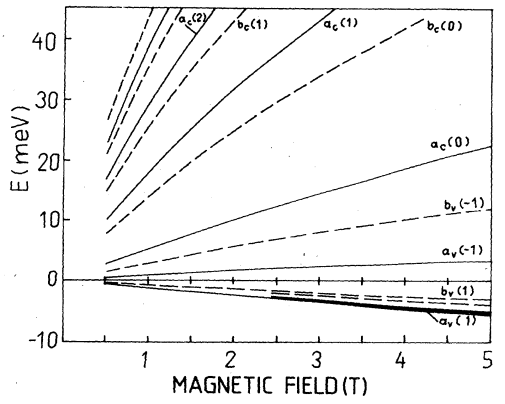

FIG. 12. Same as for Fig. 9 for $x=0.05$ (Note absence of the band overlap).

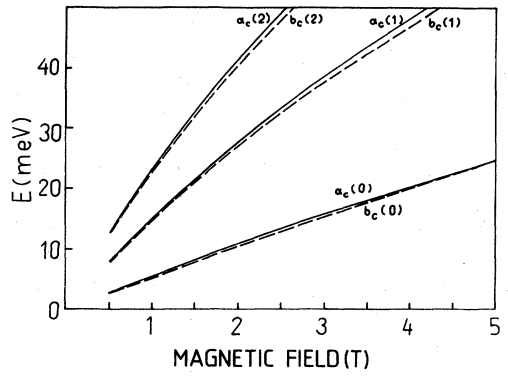

FIG. 13. Landau levels in the conduction band of the $x=0.106$ sample calculated at 5 K: a set, solid lines; b set, broken lines.

timation of the magnetization may exaggerate the shift of the $b_v(-1)$ level and this in turn may produce the band overlap in the theoretical calculation. This point shows how crucial it is to know the magnetization if the band overlap is to be studied in detail. It can be seen easily from Figs. 10—12 that for the inverted band structure the g^* factor is enhanced by the exchange interaction as compared to a nonmagnetic material. On the other hand, in the case of semiconducting band ordering ($x=0.106$ sample; Fig. 13), the exchange interaction reduces considerably the g^* factor and even causes a change in its sign as already observed in Refs. 8 and 9.

In the present paper the Kramers-Kronig analysis of the reflectivity spectra was employed to obtain the proper

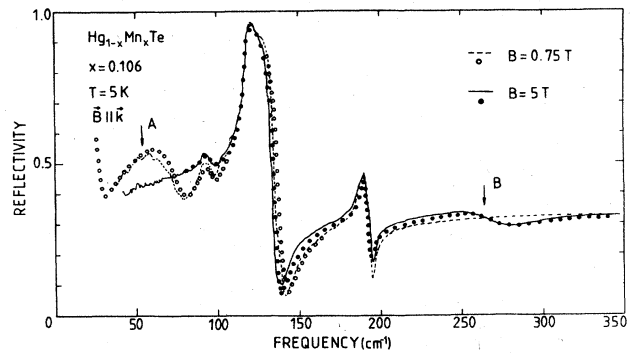

FIG. 14. Model oscillator fit (symbols) to the observed reflectivity data (lines) for $x=0.106$ sample at 5 K. The arrows A and B mark the position of the cyclotron-resonance "oscillator" for $B=0.75$ and 5 T, respectively. Fitted oscillator parameters are as follows. Electrons: $\omega_c=55$ cm^{-1}, damping $\tilde{\nu}_\tau=10$ cm^{-1} (0.75 T); $\omega_c=265$ cm^{-1}, damping $\tilde{\nu}_\tau=12$ cm^{-1} (5 T); $\omega_{p_0}=130$ cm^{-1} ($\omega^*_{p_0}=34.2$ cm^{-1}). Lattice oscillator parameters are as follows. Phonons: $\chi_\infty=13.5$; $\Delta\chi_1=0.3$, $\tilde{\nu}_{\mathrm{TO}_1}=190$ cm^{-1}, $\Gamma_1=2.5$ cm^{-1}; $\Delta\chi_2=4.35$, $\tilde{\nu}_{\mathrm{TO}_2}=117$ cm^{-1}, $\Gamma_2=1.2$ cm^{-1}; for the defect mode, $\Delta\chi_3=1$, $\tilde{\nu}_{\mathrm{def}}=95$ cm^{-1}, $\Gamma_3=8$ cm^{-1}. (In the above $\Delta\chi$'s denote the corresponding oscillators strengths and Γ's the damping parameters).

energetic position of the optical transitions. An alternative approach, as mentioned before, is based on the so-called "oscillator fit" where the values of the energies of the transitions and their strength is chosen to fit the observed reflectivity spectra. An example of such a fit is presented in Fig. 14 for $x=0.106$ sample. The values of the cyclotron-resonance frequencies obtained by this oscillator fit are in agreement with those which resulted from the Kramers-Kronig analysis of the experimental magnetoreflectivity data.

V. CONCLUSIONS

Magneto-optical properties of $Hg_{1-x}Mn_xTe$ samples with $x=0.026$, 0.035, 0.05, and 0.106 have been studied using Fourier-transform spectroscopy. A Kramers-Kronig analysis of the magnetoreflectivity spectra was performed. The magneto-optical transitions observed were interpreted in terms of the modified Pidgeon-Brown model of semimagnetic semiconductors. Direct information on the magnetization of the $x=0.026$ and 0.05 samples was obtained from an experimental determination at $T=1.9$ and 4.2 K. Using a modified Brillouin function, a good fit to the experimental values was obtained. In the case of the $x=0.106$ sample, previously measured magnetization values[23] were used; for $x=0.035$ we interpolated between all available data.[25]

The magnetic-field dependence of the observed magneto-optical transitions in Faraday as well as in Voigt geometry is properly described by the calculated transition energies and selection rules. Only some weak transitions [$a_v(-1)\rightarrow a_c(1)$ in the $\mathbf{E}\perp\mathbf{B}$ configuration in the $x=0.05$ sample and $a_v(-1)\rightarrow b_c(1)$ in the $\mathbf{E}\parallel\mathbf{B}$ configuration for the $x=0.026$ sample] are apparently not described by the usual selection rules. However, these are weakly allowed, and thus possible, due to lack of inversion symmetry in both cases and a combination of warping effects and transitions at finite k_H in the $a_v(-1)\rightarrow a_c(1)$ case.[26] The magneto-optical data show a pinning effect [also for interband transitions ($x=0.05$)] close to the LO-phonon mode energies, especially to the stronger HgTe-like mode. These pinning effects in interband transitions are more pronounced for the transitions ending at final states with low Landau quantum number, e.g., $a_c(0)$. Since information on the imaginary and real part of the dielectric function in the magnetic field was obtained, such data would be particularly suitable for a detailed analysis of the mechanism of the pinning process. However, a more detailed study of the dielectric function in the presence of a quantizing magnetic field using the proper wave functions for the free carriers in $Hg_{1-x}Mn_xTe$ would be needed.

From the good fit between calculated and experimentally observed magneto-optical transitions in all samples investigated, it is concluded that the values for the exchange parameters α and β are $\alpha=-0.4$ eV and $\beta=0.6$ eV. These are the same as used in Ref. 8 for an explanation of interband magneto-optical data for compositions $x<0.011$ and $x>0.125$.

The conduction-band and heavy-hole-band overlap [$a_c(0)-b_v(-1)$] occurring in the semimetallic composi-

tion range is found to be much less pronounced than previously expected. It still exists in $Hg_{1-x}Mn_xTe$ for a composition with $x=0.026$ at $T=5$ K but it does not occur for $x=0.035$.

ACKNOWLEDGMENTS

One of us (J.K.) would like to acknowledge the hospitality of the Montanuniversität Leoben where the greater part of this work was completed. We are grateful to Professor R. R. Galazka of the Institute of Physics, Polish Academy of Science, for growing the samples. The measurements of the magnetization and the numerical fitting of the magnetization data were done by J. A. Gaj. We thank W. Ruhs for performing the determination of the lattice constants of the samples by x-ray diffractometry and H. Krenn for help with computer programming. This work was supported by Jubiläumsfonds der Österreichischen Nationalbank, Project No. 1569, and by the Fonds zur Förderung der wissenschaftlichen Forschung, Project No. 5002.

[1]R. R. Galazka, in *Proceedings of the 14th International Conference on the Conductors, Edinburgh, 1978,* edited by B. L. H. Wilson (IOP, London, 1978), p. 133.

[2]R. R. Galazka and J. Kossut, in *Narrow Gap Semiconductors: Physics and Applications,* Vol. 133 of *Lecture Notes in Physics,* edited by W. Zawadki (Springer, Berlin, 1980), p. 245.

[3]J. A. Gaj, in Proceedings of the 15th International Conference on the Physics of Semiconductors, Kyoto, 1980 [J. Phys. Soc. Jpn. Suppl. A **49**, 747 (1980)].

[4]T. Dietl, in *Physics in High Magnetic Field,* Vol. 24 of *Springer Series on Solid State Sciences,* edited by S. Chikazumi and N. Miura (Springer, Berlin, 1981), p. 344.

[5]J. K. Furdyna, J. Appl. Phys. **53**, 7637 (1982).

[6]G. Bastard, C. Rigaux, Y. Guldner, J. Mycielski, and A. Mycielski, J. Phys. (Paris) **39**, 87 (1978).

[7]K. Pastor, M. Grynberg, and R. R. Galazka, Solid State Commun. **29**, 739 (1979).

[8]M. Dobrowolska and W. Dobrowolski, J. Phys. C **14**, 5689 (1981).

[9]G. Bastard, C. Rigaux, Y. Guldner, Y. Mycielski, J. K. Furdyna, and D. P. Mullin, Phys. Rev. B **24**, 1961 (1981).

[10]M. Grynberg, G. Martinez, and L. C. Brunel, Solid State Commun. **43**, 153 (1982).

[11]F. F. Geyer and H. Y. Fan, IEEE J. Quantum Electron. **QE-16**, 1365 (1980).

[12]S. W. McKnight, P. M. Amirtharaj, and S. Perkowitz, Solid State Commun. **25**, 357 (1978).

[13]W. Gebicki and W. Nazarewicz, Phys. Status Solidi B **80**, 307 (1977).

[14]J. Kaniewski and A. Mycielski, Solid State Commun. **41**, 959 (1982).

[15]J. Jaczynski, J. Kossut, and R. R. Galazka, Phys. Status Solidi B **88**, 73 (1978).

[16]P. Byszewski, K. Szlenk, J. Kossut, and R. R. Galazka, Phys. Status Solidi B **95**, 359 (1979).

[17]A. M. Sandauer and P. Byszewski, Phys. Status Solidi B **109**, 167 (1982).

[18]R. T. Delves and B. Lewis, J. Phys. Chem. Solids **24**, 549 (1963).

[19]L. R. Aggarwal, in *Semiconductors and Semimetals,* edited by R. K. Willardson and A. C. Beer (Academic, New York, 1972), Vol. 9, p. 151.

[20]M. H. Weiler, in *Semiconductors and Semimetals,* edited by R. K. Willardson and A. C. Beer (Academic, New York, 1981), Vol. 16, p. 119.

[21]E. D. Palik and J. K. Furdyna, Rep. Prog. Phys. **33**, 1193 (1970).

[22]M. Prasad, Phys. Status Solidi B **109**, 11 (1982).

[23]W. Dobrowolski, M. von Ortenberg, A. M. Sandauer, R. R. Galazka, and R. Pauthenet, in *Proceedings of the Fourth International Conference on the Physics of Narrow Gap Semiconductors, Linz, 1981,* Vol. 152 of *Lecture Notes in Physics,* edited by E. Gornik, H. Heinrich, and L. Palmetshofer (Springer, Berlin, 1982), p. 302.

[24]J. A. Gaj, R. Planel, and G. Fishman, Solid State Commun. **29**, 435 (1979).

[25]R. R. Galazka and J. Kossut, in *Numerical Data and Functional Relationships in Science and Technology, Group III: Crystal and Solid State Physics,* Vol. 17b of *Landolt-Börnstein, New Series,* edited by O. Madelung, M. Schulz, and H. Weiss (Springer, Berlin, 1982), p. 302.

[26]M. Weiler, Solid State Commun. **44**, 287 (1982).

[27]L. Swierkowski, W. Zawadzki, Y. Guldner, and C. Rigaux, Solid State Commun. **27**, 1245 (1978).

[28]B. L. Gelmont, V. I. Ivanov-Omskii, N. Konstantinova, D. V. Mashovets, and R. V. Parfeniev, in *Proceedings of the Third International Conference on the Physics of Narrow Gap Semiconductors, Warsaw, 1977,* edited by J. Rauluszkiewicz, M. Gorska, and E. Kaczmarek (Polish Scientific Publishers, Warszawa, 1978), p. 337.